Curie temperatures of fcc and bcc nickel and permalloy: Supercell and Green's function methods

P. Yu and X. F. Jin*,†
Surface Physics Laboratory, Fudan University, Shanghai 200433, China

J. Kudrnovský‡
Institute of Physics, Academy of Sciences of the Czech Republic, CZ-180 40 Praha 8, Czech Republic

D. S. Wang
Institute of Physics, Chinese Academy of Sciences, Beijing 100080, China

P. Bruno
Institut für Mikrostrukturphysik, Max-Planck Institut, Weinberg 2, D-06120 Halle, Germany
(Received 4 January 2007; revised manuscript received 3 January 2008; published 25 February 2008)

The finite-temperature magnetism of Ni and permalloy in body-centered-cubic (bcc) and face-centered-cubic (fcc) phases is studied theoretically using *ab initio* supercell calculations and Green's function methods. The results confirm and explain the general experimental trend that the fcc phases have higher Curie temperatures than the bcc counterparts. In addition, the spin-wave stiffness constants of bcc-Ni and bcc-permalloy are predicted.

DOI: 10.1103/PhysRevB.77.054431 PACS number(s): 75.10.Lp, 75.30.Et, 71.15.Mb

I. INTRODUCTION

The magnetism of the artificially prepared body-centered-cubic (bcc) phase of Ni has for long been an interesting topic for experimentalists.[1–4] Recently bcc-Ni was successfully prepared as a thin film on a GaAs(001) substrate using molecular beam epitaxy at 170 K, and its magnetic properties were analyzed in some detail.[5] The magnetic moments of bcc and fcc-Ni were determined to be $0.52\mu_B$ and $0.6\mu_B$, respectively. The Curie temperature of the former (456 K) was also found to be significantly lower than the latter (627 K). The bcc phase of permalloy (Py) has also been prepared using the same approach.[6] The bcc phase again has a significant lower Curie temperature (553 K) than its fcc counterpart (872 K). Here the magnetic moments are almost the same ($1.03\mu_B$ for bcc and $1.07\mu_B$ for fcc). As yet no theoretical explanation for the different Curie temperatures has been offered.

First-principles calculations of the magnetic moments have yielded the same values as found in experiments [$0.53\mu_B$ and $1.11\mu_B$ for bcc-Ni (Ref. 7) and bcc-Py,[6] respectively]. However, so far no systematic study of the finite-temperature magnetism of bcc-Ni (Ref. 8) and bcc-Py was carried out. Investigations in this field should provide additional insights to the experimentally observed trend. In addition, due to the inadequacy of the adiabatic approximation, fcc-Ni is a well known system for the existing first-principles theories have difficulties in obtaining the correct Curie temperature.[9] One of us has proposed renormalized random-phase approximation (RPA) in order to improve the quantitative agreement with the experiment.[10] The calculation of the Curie temperature of the prepared bcc-Ni represents an interesting test for this approach. Furthermore, there are few first-principles calculations of the finite-temperature magnetism of disordered alloys because of the subtlety of correctly treating the disordering effort. Given the great interest in diluted magnetic semiconductors (DMSs) this is an important problem.[11] Here a developed theory is used to investigate the disordered Ni-based magnetic alloys such as bcc- and fcc-permalloy. Finally, the spin-wave stiffness constants of both phases of Ni and permalloy are estimated from the calculated exchange parameters. The experimental verification of these predictions would lend weight to our approach.

II. THEORETICAL METHODS

First-principles calculations for the thermodynamical properties of magnetic systems are usually carried out in a two-step approach: (1) *ab initio* calculations of the total energies of the ground state and the low-lying excitations are used to determine the exchange integrals; (2) this information is used to construct the partition function from which the finite-temperature properties of the system, such as the Curie temperature, are obtained. The classical Heisenberg Hamiltonian is defined as

$$H_{\text{eff}} = -\sum_{i,j} J_{ij}\mathbf{e}_i \cdot \mathbf{e}_j, \tag{1}$$

where i is the site index, and $\mathbf{e}_i$ is the unit vector pointing along the direction of the local magnetic moment at the site i. The exchange integral J_{ij} is between magnetic atoms at sites i and j. Positive (negative) values characterize ferromagnetic (antiferromagnetic) coupling. In the case of permalloy, there are three kinds of exchange integrals $J_{i,j}^{Q,Q'}$ $(Q,Q'=\text{Ni},\text{Fe})$ corresponding to the different combinations of magnetic atoms in an alloy.

As a first step, two different first-principles methods are adopted to determine the exchange parameters for bcc- and fcc-Ni: (i) The supercell approach with full-potential linear augmented plane wave method.[12,13] In the framework of the

fixed-spin moment approach[13,14] the exchange parameters are deduced by fitting total energies of frozen collinear magnetic states of suitably chosen supercells. Here we have employed various such spin configurations in different magnetic supercells consisting of six atomic layers in one period along high-symmetry directions such as ⟨001⟩,⟨110⟩, and ⟨111⟩. As the fitting procedure is not unique, the exchange integrals vary depending on the choice of the spin configurations, despite the calculated Curie temperatures T_C are very similar. The best choice for the set of magnetic configurations for fcc structure is discussed in Ref. 14. For the bcc case, we have tested different sets of configurations and found that T_C is stable with an uncertainty of 30 K, therefore demonstrating an acceptable stability of the method with respect to the choice of the supercell and its size. (ii) The Green's function formalism using the tight-binding linear muffin-tin orbital (TB-LMTO) method.[15,16] The exchange integrals are determined from the energy changes corresponding to small rigid rotations of spins on the lattice in the framework of the adiabatic approximation.[9]

The exchange interactions of bcc- and fcc-permalloy will be estimated only with the Green's function method.[22] The Green's function approach has two important advantages for the present study. First, the theory is a simple generalization (an "inverse-susceptibility" approach[10,17]) which goes beyond the adiabatic approximation and significantly improves the calculated Curie temperatures for systems with nonrigid magnetic moments.[17] The exchange interactions in Eq. (1) do not contain contributions from constraining magnetic fields which appear as Lagrange multipliers in the constrained density-functional theory. It is perhaps justified to neglect such effects for systems with large local magnetic moments but not for the case for fcc- and bcc-Ni including Ni-rich magnetic alloys. As a consequence of nonzero constraining fields, the exchange integrals get renormalized and this is reflected in the calculated Curie temperatures. Here we use the method developed in Ref. 10 which can be conveniently combined with the RPA statistical treatment of spin fluctuations (the renormalized RPA approach). The approach has already been applied to fcc-Ni successfully.[10] However, completely satisfactory theory of the Curie temperature of magnetic systems, which takes into account both transversal and longitudinal spin fluctuations on equal footing, is still an outstanding challenge. The second advantage of the Green's function approach is that it can be also generalized to disordered alloys[18] in the framework of the coherent potential approximation (CPA).[19,20] The evaluation of the exchange integrals $J_{i,j}^{Q,Q'}$ for disordered alloys is significantly simplified by using the vertex-cancellation theorem[21] which allows us to neglect disorder-induced vertex corrections. The validity of this approximation has been tested for disordered magnetic transition metal alloys as well as diluted magnetic semiconductors (see recent review[16] for more details).

The thermodynamical property study of disordered alloys represents a complicated problem in the field of first-principles calculations. The simplest approach is to use the averaged lattice model or the virtual-crystal approximation for DMS alloys.[23] In the framework of the averaged lattice model the disordered alloy $A_{1-x}B_x$ is treated as a crystal with nonrandom effective exchange interactions.

$$J_{ij}^{eff} = (1-x)^2 J_{ij}^{AA} + x(1-x)(J_{ij}^{AB} + J_{ij}^{BA}) + x^2 J_{ij}^{BB}. \quad (2)$$

Consequently, we can directly use the mean-field approximation (MFA) as well as the renormalized RPA to estimate the Curie temperatures for crystals[15] and alloys using this effective interaction. Since this neglects magnetic percolation effects, the validity of these approximations has been questioned in recent studies[11] of DMSs. These effects are indeed relevant for diluted alloys with low concentrations of magnetic atoms in nonmagnetic hosts which have spatially well-localized exchange interactions. However, the effect of dilution is not important in permalloy with Ni concentrations well above the percolation limit. In addition, contrary to the DMSs, all sites of the alloys studied here are occupied by magnetic atoms albeit with different local moments. Finally, it was demonstrated recently that the averaged lattice model is quite successful in nondiluted disordered Ni_{2-x} MnSb Heusler alloys.[24]This supports the use of the averaged lattice model for the study of thermodynamic properties of fcc- and bcc-permalloy.

In order to lead credibility to the results, we used several different methods to determine the Curie temperatures for Ni and permalloy in both phases: (1) Monte Carlo simulation, (2) the MFA, (3) the RPA,[15] and (4) the renormalized random-phase approximation.[10,17]

The Curie temperature can be estimated from the peak in the magnetic susceptibility obtained in the Monte Carlo simulations of the classical Heisenberg model.[25] This is a conventional approach giving a reliable estimation of the Curie temperature of the systems described by the Heisenberg model. It is known[15,16] that the Curie temperatures obtained by Monte Carlo calculations and the RPA approach are in reasonable agreement for both pure and disordered systems.

However, the simplest way to obtain the Curie temperature for the Heisenberg model is to use the MFA,[15,16] i.e., from

$$k_B T_c^{MFA} = \frac{2}{3} \sum_{i \neq 0} J_{0i}. \quad (3)$$

An improved description of the finite-temperature properties is provided by the RPA and T_C is given by the following expression:

$$(k_B T_c^{RPA})^{-1} = \frac{3}{2} \frac{1}{N} \sum_{\mathbf{q}} [\mathbf{J}(\mathbf{0}) - \mathbf{J}(\mathbf{q})]^{-1}. \quad (4)$$

Here N denotes the number of $\mathbf{q}$ vectors used in the sum over the corresponding Brillouin zone, while $J(\mathbf{q})$ are the Fourier transformed real-space exchange integrals J_{ij}. It can be shown that T_c^{RPA} is smaller than T_c^{MFA}.[15,16] Finally, the Curie temperature estimated in the framework of the renormalized RPA approach is[10]

$$(k_B \tilde{T}_c^{RPA})^{-1} = (k_B T_c^{RPA})^{-1} - \frac{6}{M\Delta}, \quad (5)$$

which implies that the renormalized Curie temperature is higher compared to the bare value. Here M is the calculated local magnetic moment of the Ni atoms and Δ is the exchange splitting estimated from the difference $C_d^{\uparrow} - C_d^{\downarrow}$ of the

potential parameters C_d^σ. In the case of disordered permalloy we used the same estimate (5), but the exchange interaction (2) has to be used. For the magnetic moment M and the effective exchange splitting Δ it is important to note that in Eq. (5) we used virtual-crystal averages, namely, $X=(1-x)X^A+xX^B$ ($X=M$, or Δ), for the case of random alloy. Such a choice seems to be obvious for the averaged lattice model, consistent with Eq. (2), although to date we are not able to give a better justification. The corresponding theory of renormalized RPA for random alloys is still to be developed.

In the statistical study we have used 231 and 246 shells for fcc-, bcc-Ni, and permalloy which we have tested for convergence with respect to the number of shells. The estimated computational error corresponding to the limited number of shells used in calculations is below ± 5 K.

The spin-wave stiffness constant D is given by the curvature of the spin-wave dispersion at $\mathbf{q}=0$. In terms of exchange integrals it can be defined directly in real space as[9,15,16]

$$D = \frac{2}{3M}\sum_{i\neq 0} J_{0i}R_{0i}^2, \tag{6}$$

where R_{0i} is the distance between lattice sites i and j. Although the calculation of D is straightforward, serious difficulties arise due to the fact that the lattice sum is not absolutely convergent and exhibits undamped oscillations with respect to the number of shells included in the summation.[15] These oscillations are suppressed by the introduction of exponentially damped terms in Eq. (6). The lattice sum is absolutely convergent and the spin-wave stiffness constant D can be estimated by a quadratic least-square interpolation method from the set of calculated values. For technical details concerning this method we refer the reader to Ref. 15. We also used the averaged lattice model for the evaluation of the spin-wave stiffness constants of fcc- and bcc-permalloy.

III. RESULTS AND DISCUSSION

For fcc-Ni and fcc-permalloy the lattice constants were chosen to be 3.52 and 3.55 Å, while for bcc systems the lattice constant corresponds to the experimental values ($a=2.825$ Å). In the present work the composition of the permalloy is $Ni_{0.75}Fe_{0.25}$. Calculated local magnetic moments of fcc- and bcc-Ni ($M_{fcc}=0.63\mu_B$ and $M_{bcc}=0.53\mu_B$) agree well with experimental values ($M_{fcc}=0.60\mu_B$ and $M_{fcc}=0.52\mu_B$) and also fit well with other recent theoretical studies.[7,8]

Exchange integrals of bcc- and fcc-Ni, for the supercell and Green's function method, are summarized in Figs. 1 and 2. It should be kept in mind that the supercell method only allows us to extract a limited set of exchange integrals in contrast with the Green's function approach. From this point of view there is a reasonable agreement of calculated exchange integrals for both approaches. The exchange integrals $J^{Ni,Ni}$ dominate the first nearest-neighbor interactions in both phases. These are more localized in real space for fcc-Ni than bcc-Ni (see Fig. 2). This can be understood qualitatively with the help of the corresponding density of states in Fig. 3. The Fermi level in the gap of majority or minority states

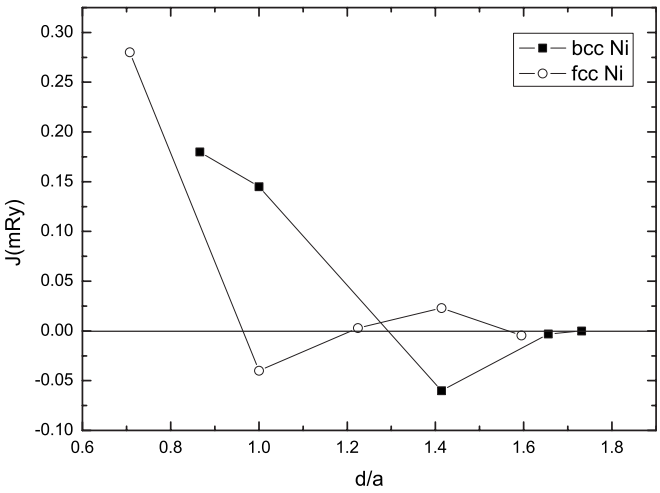

FIG. 1. Exchange interactions for fcc- and bcc-Ni as a function of the distance between two spins obtained by fitting to the frozen collinear spin configurations.

leads to exponentially damped exchange integrals.[15,24] The density of states in fcc-Ni, at the Fermi level, for majority spins is not zero but very low (sp states), while in the bcc phase the Fermi level is located in the d band for both spin orientations. This is related to the fact that fcc-Ni is a strong ferromagnet while bcc-Ni is a weak ferromagnet similar to bcc-Fe. Despite the fact that the values of exchange integrals seem to be comparable for both bcc- and fcc-Ni, a higher T_C for fcc-Ni can be expected since the coordination number is larger than that of the bcc lattice. This is obvious from a simple mean-field estimation of the Curie temperature and it has been confirmed by calculations going beyond the MFA (see Table I).

Calculated Curie temperatures for fcc- and bcc-Ni are summarized in Table I. As we have already mentioned Ni represents a difficult case in both phases due to its small and soft magnetic moment which violates the adiabatic approximation.[10,17] Furthermore, correlation effects and Stoner excitations have been neglected. As it was demon-

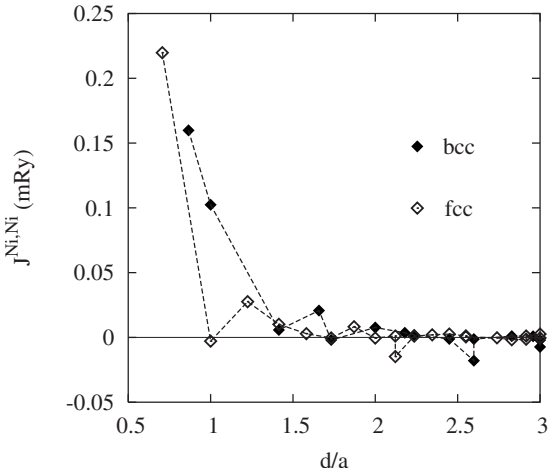

FIG. 2. Exchange interactions of fcc- and bcc-Ni as a function of the distance between two spins calculated in the framework of the TB-LMTO method.

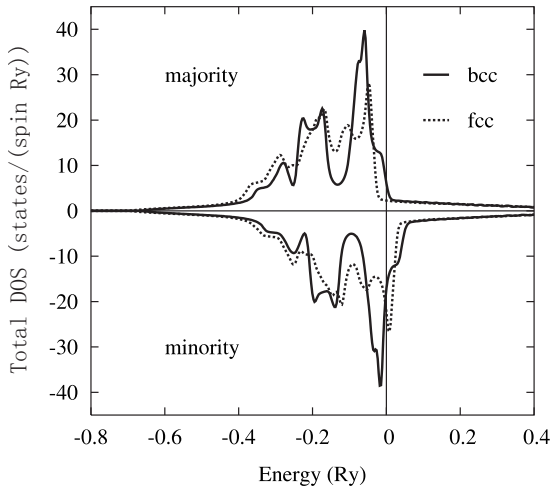

FIG. 3. Spin-polarized density of states for fcc- and bcc-Ni calculated in the framework of the TB-LMTO method.

strated by Bruno[10] for fcc-Ni, the violation of the adiabatic approximation seems to be of central importance. We have therefore used the renormalized RPA theory, in addition to the conventional MFA, RPA, and Monte Carlo (MC) estimates of T_C, to bring the calculated Curie temperatures into a better quantitative agreement with the experimental data[26] (see Table I). For both phases the MFA, conventional RPA, as well as MC approaches all underestimate T_C. Among these three methods, the MFA provides a seemingly better agreement with the experiment despite the fact that the MFA is a better theory for high Curie temperatures.

While the agreement between calculated T_C for fcc-Ni and the experimental value is quite good in the framework of the renormalized RPA, the calculated T_C for bcc-Ni is still underestimated by about 50%. Ni is a narrow band transition metal that implies correlation effects are important. We have addressed this question by applying the LDA+U method[27] in the framework of the Green's function approach. We used the Hubbard parameters $U=0.16$ Ry and $J=0.06$ Ry. The calculated magnetic moment of bcc-Ni is only slightly enhanced from $0.53\mu_B$ to $0.59\mu_B$. The Curie temperature T_C increases substantially from 286 to about 380 K. While this is still smaller than the experimental T_C, the agreement is now reasonable. On the other hand, the fcc-Ni seems to be less sensitive to correlation effects. For the same U and J parameters as for bcc-Ni, the magnetic moment of fcc-Ni only increases from $0.631\mu_B$ to $0.688\mu_B$. The Curie temperature of 686 K increases weakly to 690 K in the remormalized RPA approach. The present calculations can only be taken as indication of the influence of electron correlations on T_C. However, more systematic studies are needed. Also Stoner excitations have been neglected and these could play a different role in fcc- and bcc-Ni crystals and therefore need to be investigated in more detail. Finally, we have also neglected possible tetragonal deformations of the lattice in the growth direction of Ni films on GaAs substrate. This only slightly modifies the calculated values of the Curie temperature.[8]

TABLE I. Curie temperatures T_C (in K) of fcc- and bcc-Ni obtained by different methods: supercell-Monte Carlo method (T_C^{MC}) and the Green's function approach in the framework of the mean-field approximation (T_C^{MFA}), the random-phase approximation (T_C^{RPA}), and in the renormalized random-phase approximation ($\tilde{T}_C^{RPA}$) (see text for definitions). The experimental values (T_C^{expt}) are also shown.

System	T_C^{MC}	T_C^{MFA}	T_C^{RPA}	$\tilde{T}_C^{RPA}$	T_C^{expt}
bcc-Ni	115	250	190	286	456
fcc-Ni	300	413	369	686	627

A. fcc- and bcc-permalloy

The calculated averaged magnetic moments of fcc- and bcc-Py ($M_{fcc}=1.12\mu_B$ and $M_{bcc}=1.09\mu_B$) agree well with the experimental values ($M_{fcc}^{expt}=1.07\pm0.09\mu_B$ and $M_{bcc}^{expt}=1.03\pm0.09\mu_B$).[6] Theoretical values obtained by CPA calculation also agree well with the values obtained by the supercell approach ($M_{fcc}=1.14\mu_B$ and $M_{bcc}=1.1\mu_B$).[6] The Calculated local moments of Ni atoms in fcc-Py and bcc-Py are almost the same as in corresponding pure crystals ($M_{fcc}^{Ni}=0.63\mu_B$ and $M_{bcc}^{Ni}=0.57\mu_B$). The local moments on "impurity" Fe atoms in bcc-Py are enhanced compared with the bulk bcc-Fe ($M_{bcc}^{Fe}=2.67\mu_B$ and $M_{bulk}^{Fe}=2.15\mu_B$) despite the fact that the Py-lattice constant is slightly compressed compared with bulk Fe. This reflects the filling of the partially occupied majority Fe bands by Ni electrons in the permalloy composition. The Fe-majority states are already filled [see Fig. 4(b)]. This leads to an enhanced Fe moment.

The total and local densities of states (DOSs) in fcc and bcc phases of Py are shown in Figs. 4(a) and 4(b). The behavior of corresponding Ni- and Fe-resolved local DOSs can be understood from the alloy level data shown in Table II. We identify atomic levels with values of the corresponding potential parameters $C_d^{Q,\sigma}$, where Q=Ni, Fe, and $\sigma=\uparrow,\downarrow$.[19] In addition, values for the nonmagnetic alloys are given for comparison. Three relevant facts have to be mentioned: (i) Nonmagnetic Fe d levels are higher than corresponding Ni levels; (ii) because of larger local moments, Fe d-atomic levels split more than Ni levels and (iii) Fe bandwidths are larger than Ni bandwidths. The above mentioned features are common for both fcc- and bcc-Py. An immediate consequence of these facts is a significantly smaller difference between majority atomic levels and minority ones. As a result, there is a strong level disorder for minority spin electrons but only a weak disorder for majority ones, in particular, for fcc-permalloy. We note that the local DOS is dominated by d bands of canonical shape which differ only in their widths and hybridization with sp electrons. As a consequence, for majority bands the component local DOSs are very similar with negligible disorder and they resemble the DOS of the corresponding host Ni metal (compare Fig. 3). Although Fe bands are a little broader, the widths of Fe and Ni local DOSs are quite similar especially for fcc-Py. This is due to the fact that Fe atoms are impurities in random alloy and therefore have a reduced bandwidths.[19] The situation is completely different for minority spin states which

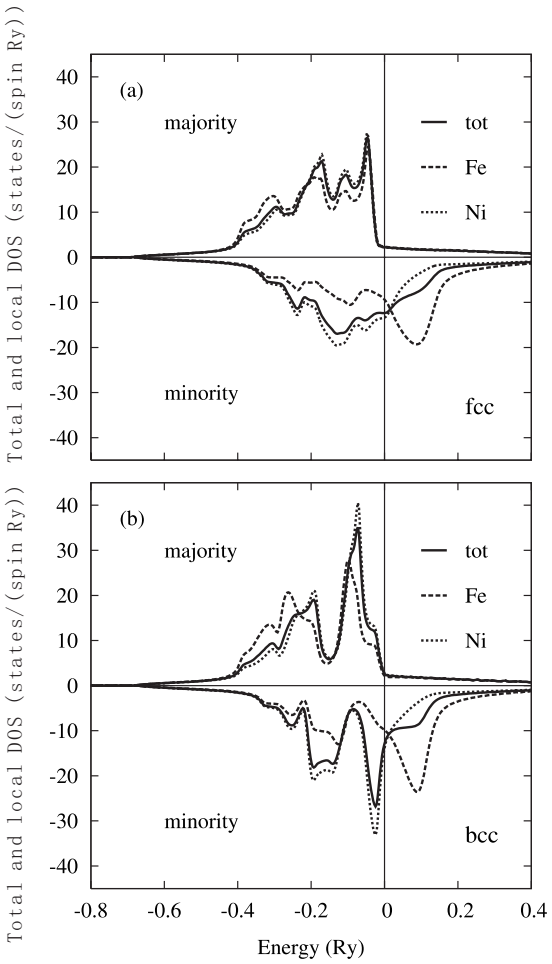

FIG. 4. Spin-polarized density of states calculated in the framework of the TB-LMTO method: (a) fcc-permalloy for which both total and species-resolved (Ni and Fe) local densities of states are shown; (b) the same as in (a) but for bcc-permalloy.

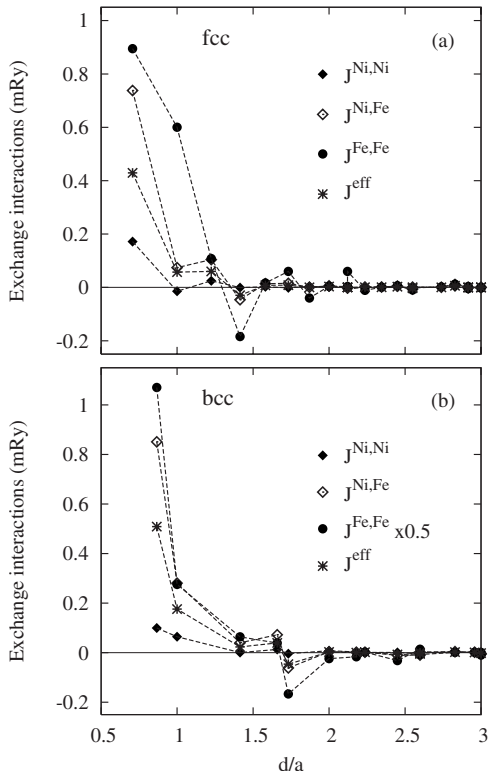

FIG. 5. Exchange interactions $J^{QQ'}$ $(Q,Q'=\mathrm{Ni,Fe})$ as a function of the distance between two spins calculated in the framework of the TB-LMTO method: (a) fcc-permalloy for which the effective interactions J^{eff}, Eq. (2), are also shown; (b) the same as in (a) but for bcc-permalloy. Note that the $J^{\mathrm{Fe,Fe}}$ interactions are reduced by a factor of 2.

have a strong level disorder. In this case Fe and Ni states are clearly separated in energy and their shapes are also modified by disorder, especially for the impurity (Fe) constituent. The minority spin levels are also higher in energy than majority ones, which are bound by alloy potential more weakly. As a result, minority bandwidths are larger than majority ones. Such a different behavior of majority and minority spin states in magnetic transition metal alloys was also found in the other systems (see, e.g., Ref. 28).

The effect of disorder can be very different in different energy regions. To illustrate this more quantitatively, we have evaluated the residual resistivity using the Kubo-Greenwood formula implemented in the framework of the TB-LMTO method[29] which can serve as a simple probe of the strength of impurity scattering at the Fermi energy. The Fermi energy also plays an important role in the determination of exchange integrals. The calculated residual resistivities of fcc- and bcc-Py (0.69 and 0.05 $\mu\Omega$ cm) clearly illustrate the weaker impurity scattering in bcc-Py at the Fermi energy. We estimate the absence of the disorder-induced vertex corrections lowers the calculated resistivities by about 10% in both cases. However, the calculated resistivities solely illustrate the different scattering strengths of Fe impurities in fcc- and bcc-Py at the Fermi energy. The spin-orbit coupling, neglected here, couples weak-scattering majority channels with the strong-scattering minority channels and leads to a significantly larger resistivity.[30]

Calculated exchange interactions in fcc- and bcc-Py are shown in Figs. 5(a) and 5(b). Exchange interactions between pairs of Ni atoms in fcc-Py are almost the same as in the pure

TABLE II. Alloy level data of the ferromagnetic bcc- and fcc-permalloy. Atomic levels $(Q=\mathrm{Ni,Fe})$ are indentified with potential parameters $C_d^{Q,\sigma}$ $(\sigma=\uparrow,\downarrow)$ of the LMTO theory. Corresponding values for nonmagnetic case, $C_d^{Q,\sigma}$, are also shown. All values are in Ry.

System	C_d^{Ni}	C_d^{Fe}	$C_d^{\mathrm{Ni},\uparrow}$	$C_d^{\mathrm{Fe},\uparrow}$	$C_d^{\mathrm{Ni},\downarrow}$	$C_d^{\mathrm{Fe},\downarrow}$
fcc Py	−0.185	−0.143	−0.192	−0.212	−0.145	−0.034
bcc Py	−0.180	−0.142	−0.194	−0.236	−0.149	−0.050

TABLE III. Curie temperatures T_C (in K) of fcc- and bcc-permalloy in the averaged lattice approximation obtained by different methods in the framework of the Green's function approach: the mean-field approximation (T_C^{MFA}), the random-phase approximation (T_C^{RPA}), and the renormalized random-phase approximation ($\tilde{T}_C^{RPA}$) (see text for their definitions). The experimental values (T_C^{expt}) are also shown, two different ones for fcc-permalloy.

System	T_C^{MFA}	T_C^{RPA}	$\tilde{T}_C^{RPA}$	T_C^{expt}
bcc-Py	605	466	586	553
fcc-Py	723	608	812	871(858)

fcc-Ni (compare Fig. 2). The effective interactions in fcc-Py are enhanced in comparison with the interactions in pure fcc-Ni due to Fe-Ni interactions. The Fe-Fe exchange interactions are larger, as expected, but their weight in the effective interaction is rather small in the Ni-rich $Fe_{0.25}Ni_{0.75}$ disordered alloy. The enhancement is particularly large for the first nearest-neighbor interactions which dominate the MFA Curie temperature. The dependence of the effective exchange interactions on the distance has almost the same behavior as in the pure fcc-Ni. The increase of the effective exchange interactions is caused by the alloying with Fe atoms and is a direct reason for the higher Curie temperature of fcc-Py. The larger spatial extent of the Fe-Fe pair interactions compared with the Fe-Ni and Ni-Ni and their oscillatory character both relate to the partially filled minority states [see Fig. 4(a)].

The character of effective exchange interactions in bcc-Py is similar to those in the pure bcc-Ni. Again the exchange interactions are also enhanced by the presence of Fe atoms. The Fe-Fe pair interaction in bcc-Py dominates and is similar in character to that of pure bcc-Fe.[15] The value is actually larger than in pure bcc-Fe due to enhanced local magnetic moments (larger exchange splitting) of Fe atoms in bcc-Py. Despite the fact that the effective exchange interactions in bcc-Py are comparable to those in fcc-Py, bcc-Py has a lower Curie temperature because of its fewer first nearest neighbors.

The calculated Curie temperatures of fcc- and bcc-Py in the framework of the averaged lattice model under different approximations are summarized in Table III. It is obvious that only the renormalized RPA method provides values in fair agreement with experiment. It seems that the averaged lattice model represents an acceptable approximation for Ni-rich permalloy. While absolute values of Ni and permalloy Curie temperatures match with the experiment, their relative differences are less satisfactorily. The reason is that the bcc-Ni Curie temperature is underestimated in the present calculations while Curie temperature for bcc-Py is overestimated. For fcc-Ni and fcc-Py the situation is similar but reversed. Although there is no clear explanation at the moment, it is possible that the averaged lattice model for disordered alloys underestimates the effect of large exchange interactions between Fe atoms in bcc-Py. In addition, the renormalized RPA can influence the calculated T_C in fcc and bcc phases differently.

One can also speculate about the concentration dependence of the Curie temperature for bcc-$Ni_{1-x}Fe_x$ alloys. A relatively high Curie temperature close to that of the pure bcc-Fe (1040 K) and it can be expected to increase monotonically with the Fe concentration. The case studied here ($x=0.25$) confirms this trend. For the fcc counterpart, the situation is known: There is a well-pronounced maximum of the Curie temperature at about $x=0.25$. For the Fe-rich end the situation is quite complicated since the ferromagnetic fcc phase exists only up to about $x<0.8$.

TABLE IV. Calculated spin-wave stiffness constants D_{th} (in meV Å^2) and estimated error bars (in parentheses). The experimental values D_{expt} for fcc phases of Ni and Py are also shown.

	fcc-Ni	bcc-Ni	fcc-Py	bcc-Py
D_{th}	755(25)	170(15)	515(10)	295(10)
D_{expt}	555,530(20)		370(10)	

B. Spin-wave stiffness constants

The calculated spin-wave stiffness constants together with available experimental data are summarized in Table IV. The estimated error bars correspond to various sets of damping parameters η used for the least-square fit as described above. Experimental results are known only for fcc-Ni (Refs. 31 and 32) and fcc-permalloy.[32] In general, the values of the spin-wave stiffness constant are strongly reduced with the temperature[31] and we therefore compare theoretical estimates with available low-temperature measurements.

Calculated spin-wave stiffness constant for fcc-Ni agree well with a related approach in which it is determined by the second derivative of the calculated spin-wave spectrum.[33] However, the theoretical value is overestimated compared with the experiment. On the other hand, the reduction of the spin-wave stiffness constant due to alloying Ni with Fe atoms is reproduced quite well. Although the spin-stiffness constant of fcc-Py is also overestimated compared with the experiment, the ratio $D(\mathrm{Ni}):D(\mathrm{Py})$ is calculated correctly.

There are no experimental data for the spin-wave stiffness D of bcc-Ni and bcc-permalloy. The calculated spin-wave stiffness of bcc-Ni is comparable in its size to that of bcc-Fe (250–280 meV Å^2). but significantly smaller than that of fcc-Ni which is due to its reduced number of exchange integrals at a given distance.[15,33] The same qualitative explanation is also valid for T_C but here the effect is stronger due to a factor R_{ij}^2 in Eq. (6). The evaluation of the spin-stiffness constant is a more delicate problem than that of the Curie temperature and the results are also more sensitive with regarding to the details of the calculations. The spin-wave stiffness constant of bcc-Py is larger than that of bcc-Ni. We have shown that the effect of electron correlations can be important for bcc-Ni, so D was also evaluated in the framework of the LDA+U approach. While the spin-wave stiffness constant of fcc-Ni is influenced by correlations weakly (690 ± 20 meV Å^2). the corresponding change for bcc-Ni is large (350 ± 15 meV Å^2). It would be interesting to obtain the values of D from experiment for the bcc phases and compare them with the theoretically present predictions.

We can conclude that the state-of-the-art first-principles calculations give correct qualitative explanation of observed magnetic properties of artificially prepared bcc phases of Ni and permalloy samples. Results have been compared with conventional fcc phases of both materials and can be summarized as follows: (i) Calculated magnetic moments agree very well with experimental data for both phases and materials; (ii) the parameter-free theory explains observed higher Curie temperatures of fcc phases of Ni and permalloy in comparison with their bcc counterparts, and even a satisfying quantitative agreement between all calculated Curie temperatures and experimental values. Except for bcc-Ni, the agreement of calculated and measured Curie temperatures is better than 10% which is the present accuracy of parameter-free approaches. (iii) We have also clearly demonstrated that the renormalized RPA approach, which goes beyond the adiabatic approximation, is needed for a good quantitative agreement with experiment. (iv) These results suggest that the averaged lattice model is a reasonable approximation for the calculation of the Curie temperatures of concentrated magnetic alloys. Lastly, (v) the calculated ratio of spin-wave stiffness constants of fcc-Ni and fcc-permalloy are in good agreement with experiments although their absolute values are too large.

Ni and Ni-rich magnetic alloys still represent a challenge for theory, in particular, for *ab initio* studies. The effect of Stoner excitations as well as electron correlations should be investigated in more detail in the future to improve quantitative agreement between the theory and experiments.

ACKNOWLEDGMENTS

X.F.J. acknowledges the financial support of the Natural Science Foundation of China, the 973 project under Grant No. 2006CB921303 of the Science and Technology Ministry of China, the Ministry of Education of China for Ph.D. Training, and the Shanghai Science and Technology Committee. J.K. acknowledges the financial support from the Grant Agency of the Academy Sciences of the Czech Republic (A100100616) and COST P19 (OC150).

*Authors to whom correspondence should be addressed
†xfjin@fudan.edu.cn
‡kudrnov@fzu.cz

[1] Q. Wang, Y. S. Li, F. Jona, and P. M. Marcus, Solid State Commun. **61**, 623 (1987).
[2] B. Heinrich, S. T. Purcell, J. R. Dutcher, K. B. Urquhart, J. F. Cochran, and A. S. Arrott, Phys. Rev. B **38**, 12879 (1988).
[3] Z. Celinski, K. B. Urquhart, and B. Heinrich, J. Magn. Magn. Mater. **166**, 6 (1997).
[4] N. B. Brookes, A. Clarke, and P. D. Johnson, Phys. Rev. B **46**, 237 (1992).
[5] C. S. Tian, D. Qian, D. Wu, R. H. He, Y. Z. Wu, W. X. Tang, L. F. Yin, Y. S. Shi, G. S. Dong, X. F. Jin, X. M. Jiang, F. Q. Liu, H. J. Qian, K. Sun, L. M. Wang, G. Rossi, Z. Q. Qiu, and J. Shi, Phys. Rev. Lett. **94**, 137210 (2005); W. X. Tang, D. Qian, D. Wu, Y. Z. Wu, G. S. Dong, X. F. Jin, S. M. Chen, X. M. Jiang, X. X. Zhang, and Z. Zhang, J. Magn. Magn. Mater. **240**, 404 (2002).
[6] L. F. Yin, D. H. Wei, N. Lei, L. H. Zhou, C. S. Tian, G. S. Dong, X. F. Jin, L. P. Guo, Q. J. Jia, and R. Q. Wu, Phys. Rev. Lett. **97**, 067203 (2006).
[7] G. Y. Guo and H. H. Wang, Chin. J. Phys. (Taipei) **38**, 949 (2000).
[8] S. Khmelevskyi and P. Mohn, Phys. Rev. B **75**, 012411 (2007). In this very recent paper devoted to the structural and magnetic properties of bcc-Ni is also given a simple mean-field estimate of its Curie temperature.
[9] A. I. Liechtenstein, M. I. Katsnelson, V. P. Antropov, and V. A. Gubanov, J. Magn. Magn. Mater. **67**, 65 (1987).
[10] P. Bruno, Phys. Rev. Lett. **90**, 087205 (2003).
[11] L. Bergqvist, O. Eriksson, J. Kudrnovský, V. Drchal, P. Korzhavyi, and I. Turek, Phys. Rev. Lett. **93**, 137202 (2004); K. Sato, W. Schweika, P. H. Dederichs, and H. Katayama-Yoshida, Phys. Rev. B **70** 201202(R) (2004); G. Bouzerar, T. Ziman, and J. Kudrnovský, Europhys. Lett. **69**, 812 (2005).
[12] N. M. Rosengaard and B. Johansson, Phys. Rev. B **55**, 14975 (1997).
[13] Y.-M. Zhou, D.-S. Wang, and Y. Kawazoe, Phys. Rev. B **59**, 8387 (1999).
[14] X. Gao, Y. M. Zhou, and D. S. Wang, J. Magn. Magn. Mater. **251**, 29 (2002).
[15] M. Pajda, J. Kudrnovský, I. Turek, V. Drchal, and P. Bruno, Phys. Rev. B **64**, 174402 (2001).
[16] I. Turek, J. Kudrnovský, V. Drchal, and P. Bruno, Philos. Mag. **86**, 1713 (2006).
[17] V. I. Antropov, J. Magn. Magn. Mater. **262**, L192 (2003); M. I. Katsnelson and A. I. Liechtenstein, J. Phys.: Condens. Matter **16**, 7439 (2004).
[18] J. Kudrnovský, I. Turek, V. Drchal, F. Máca, P. Weinberger, and P. Bruno, Phys. Rev. B **69**, 115208 (2004).
[19] I. Turek, V. Drchal, J. Kudrnovský, M. Šob, and P. Weinberger, *Electronic Structure of Disordered Alloys, Surfaces and Interfaces* (Kluwer, Boston, 1997).
[20] I. Turek, J. Kudrnovský, and V. Drchal, in *Electronic Structure and Physical Properties of Solids*, Lecture Notes in Physics Vol. 535 edited by H. Dreyssé (Springer, Berlin, 2000), p. 349.
[21] P. Bruno, J. Kudrnovský, V. Drchal, and I. Turek, Phys. Rev. Lett. **76**, 4254 (1996).
[22] L. M. Sandratskii and P. Bruno, Phys. Rev. B **66**, 134435 (2002).
[23] T. Dietl, H. Ohno, and F. Matsukura, Phys. Rev. B **63**, 195205 (2001).
[24] J. Rusz, L. Bergqvist, J. Kudrnovský, and I. Turek, Phys. Rev. B **73**, 214412 (2006).
[25] *Monte Carlo Simulation in Statistical Physics*, edited by K. Binder and D. W. Heermann (Springer-Verlag, Berlin, 1988).
[26] Slightly different values of T_C^{RPA} and $\tilde{T}_C^{RPA}$ for fcc-Ni in the present paper and in Ref. 10 are due to the use of the scalar-relativistic and nonrelativistic TB-LMTO approaches, respectively.
[27] Alexander B. Shick, Josef Kudrnovsky, and Vclav Drchal, Phys.

Rev. B **69**, 125207 (2004).
[28] I. Turek, J. Kudrnovský, V. Drchal, and P. Weinberger, Phys. Rev. B **49**, 3352 (1994).
[29] I. Turek, J. Kudrnovsky, V. Drchal, L. Szunyogh, and P. Weinberger, Phys. Rev. B **65**, 125101 (2002).
[30] D. M. Nicholson, W. H. Butler, W. A. Shelton, Yang Wang, X.-G. Zhang, and G. M. Stocks, J. Appl. Phys. **81**, 4023 (1997).
[31] H. A. Mook, J. W. Lynn, and R. M. Nicklow, Phys. Rev. Lett. **30**, 556 (1973).
[32] D. Bonnenberg, K. A. Hempel, and H. P. J. Wijn, *Lanhold-Börnstein — Group III Condensed Matter: Numerical Data and Functional Relationships in Science and Technology*, Landolt-Börnstein, New Series III/19a (Springer, Berlin, 1986).
[33] M. van Schilfgaarde and V. P. Antropov, J. Appl. Phys. **85**, 4827 (1999).